
Research Article: New Research | Cognition and Behavior

Threat anticipation in pulvinar and in superficial layers of primary visual cortex (V1). Evidence from layer-specific ultra-high field 7T fMRI

<https://doi.org/10.1523/ENEURO.0429-19.2019>

Cite as: eNeuro 2019; 10.1523/ENEURO.0429-19.2019

Received: 14 October 2019

Accepted: 17 October 2019

This Early Release article has been peer-reviewed and accepted, but has not been through the composition and copyediting processes. The final version may differ slightly in style or formatting and will contain links to any extended data.

Alerts: Sign up at www.eneuro.org/alerts to receive customized email alerts when the fully formatted version of this article is published.

Copyright © 2019 Koizumi et al.

This is an open-access article distributed under the terms of the Creative Commons Attribution 4.0 International license, which permits unrestricted use, distribution and reproduction in any medium provided that the original work is properly attributed.

1

Pulvinar and V1 in threat anticipation

2

3 Threat anticipation in pulvinar and in superficial layers of primary visual cortex (V1). Evidence from layer-
4 specific ultra-high field 7T fMRI.

5

6 Ai Koizumi^{1,2,3,4*}, Minye Zhan⁵, Hiroshi Ban^{1,2}, Ikuhiro Kida^{1,2}, Federico De Martino⁵, Maarten J. Vaessen⁵,
7 Beatrice de Gelder^{5, 6*}, Kaoru Amano^{1,2}

8

9 1. Center for Information and Neural Networks (CiNet), National Institute of Information and Communications
10 Technology (NICT)

11 2. Graduate School of Frontier Biosciences, Osaka University

12 3. Sony Computer Science Laboratories, Inc.

13 4. Graduate School of Media and Governance, Keio University

14 5. Department of Cognitive Neuroscience, Maastricht University

15 6. Department of Computer Science, UCL

16

17 **Author Contributions:** AK, HB, BDG, and KA contributed to the study design, FDM and IK contributed to the
18 scanning and parameter settings of 7T fMRI, AK and MZ collected the data, AK conducted the data analyses with
19 guidance and feedback from FDM, MZ, HB, MV and KA. AK, KA, and BDG wrote the manuscript with feedback from
20 HB, MZ, FDM, and IK.

21

22 **Correspondence should be addressed to:** Ai Koizumi (bellkoizumi@gmail.com) & Beatrice de Gelder
23 (b.degelder@maastrichtuniversity.nl)

24

25 Number of Figures: 4, Number of Tables: 1, Number of Multimedia: 0

26 Number of words for Abstract: 183, Number of words for Significance Statement: 103

27 Number of words for Introduction: 749, Number of words for Discussion: 1313

28

29

30

31

Acknowledgements

33 This research was funded by a European Research Council (ERC) grant under the European 512 Union
34 Seventh Framework Programme for Research 2007–2013 (grant agreement number 513 295673),
35 European Union’s Horizon 2020 Research and Innovation Programme under grant 514 agreement No
36 645553, ICT DANCE (IA, 2015-2017), Incentive grant of National Institute of Information and
37 Communications Technology (NICT), Japan, JSPS KAKENHI grant number 16K21687 and 18H02714
38 awarded to AK, and ERATO (JPMJER1801) awarded to HB. The funders had no role in study design,
39 data collection and analysis, decision to publish, or preparation of the manuscript. We thank Prof. Yuka
40 Sasaki, Prof. Ben Seymour, Dr. Kazuhisa Shibata, Prof. Nim Tottenham, Dr. Brian Maniscalco, and Dr.
41 Jorge Morales for their useful comments.

42

43 **Conflict of Interest:** No. Authors report no conflict of interest

44

45 **Funding sources:** Please find information in Acknowledgement.

46

47

Abstract

48 The perceptual system gives priority to threat-relevant signals with survival value. In addition to the
49 processing initiated by sensory inputs of threat signals, prioritization of threat signals may also include
50 processes related to threat anticipation. These neural mechanisms remain largely unknown. Using ultra-
51 high-field 7T fMRI, we show that anticipatory processing takes place in the early stages of visual
52 processing, specifically in the pulvinar and V1. When anticipation of a threat-relevant fearful face target
53 triggered false perception of not-presented target, there was enhanced activity in the pulvinar as well as
54 in the V1 superficial-cortical-depth (layers 1–3). The anticipatory activity was absent in the LGN or higher
55 visual cortical areas (V2-4). The effect in V1 was specific to the perception of fearful face targets and did
56 not generalize to happy face targets. A preliminary analysis showed that the connectivity between the
57 pulvinar and V1 superficial-cortical-depth was enhanced during false perception of threat, indicating that
58 the pulvinar and V1 may interact in preparation of anticipated threat. The anticipatory processing
59 supported by the pulvinar and V1 may play an important role in non-sensory-input driven anxiety states.

60

61 **Keywords:** threat perception; fearful face; 7 Tesla fMRI; V1 cortical layer, pulvinar

83

Introduction

84 Fear and anxiety are core states of the organism and understanding these is a central issue for
85 neuroscience. The importance of these psychological states is highlighted by findings that the visual
86 system prioritizes inputs with high behavioural relevance (Bishop, 2007) such as threat signals from facial
87 or bodily expression (Lanzetta and Orr, 1986; de Gelder, 2006; Koizumi et al., 2016). Fear is triggered by
88 actual threat signals, but threat stimuli can also be anticipated and induce fear as is typically the case in
89 anxiety (Grillon et al., 2017; Torrisi et al., 2018). The neural mechanisms underlying such anticipatory
90 processing of threat, however, remains largely unknown.

91 We here hypothesize that when threat is anticipated, activity changes are seen in the early stage
92 of visual processing in the pulvinar and V1. The literature postulates the pulvinar as a central relay,
93 forwarding threat-relevant sensory inputs to other cortical and subcortical areas for quick evaluation and
94 response (LeDoux, 1996; Pessoa and Adolphs, 2010; Tamietto and de Gelder, 2010; McFadyen et al.,
95 2017). In addition to input-driven processing, the pulvinar is also known to receive inputs from higher
96 cortex including prefrontal areas (Grieve et al., 2000; Bridge et al., 2016) presumably contributing to
97 higher-level perceptual processing (Saalmann and Kastner, 2011; Kanai et al., 2015; Roth et al., 2016). In
98 addition, we hypothesize that anticipatory processing of threat may involve the earliest stage of visual
99 cortical hierarchy, V1. Studies using simple visual stimuli such as gratings have shown that V1 activity
100 reflects not only the physically presented stimuli but also the subjective perception as in the case of false
101 alarm (Ress and Heeger, 2003; Pajani et al., 2015). Relatedly, a recent study has demonstrated that
102 visual images that are not physically present, but are well expected from the surrounding scenes, can
103 induce the expected-image-like activity in V1 (Muckli et al., 2015). This effect was observed specifically in
104 its superficial layers known to be modulated by the pulvinar in non-human primates (Shipp, 2003, 2007).
105 These results suggest an active role of V1, especially its superficial cortical depth, in shaping visual
106 perception in a top-down manner, at least when guided by some sensory inputs (Muckli et al., 2015).

107 To examine the role of the pulvinar and V1 in threat anticipation we designed an experiment
108 where participants performed a simple task to detect a fearful face target (**Fig. 1**), which served as a
109 social threat signal (Lanzetta and Orr, 1986; de Gelder, 2006). In a separate control session, a happy
110 face detection task allowed us to examine whether the pulvinar and/or V1 contribute specifically to

111 anticipation of threat or generalizes to any salient target. Importantly, participants were informed which
112 target would be presented prior to each session in order to build their anticipation of a given target (Pajani
113 et al., 2015). Prior knowledge combined with weakened sensory input due to brief presentation, induced
114 participants' anticipation leading to more false percepts (Friston, 2005; Pajani et al., 2015). In each
115 session, half of the trials randomly presented target faces (fearful or happy) and half neutral faces.
116 Participants falsely perceived either a fearful or happy face target when a neutral face was actually
117 presented in approximately 25% of the cases. We hypothesize that, unlike the trials where participants
118 correctly perceive the presented fearful faces (i.e., HIT trials), the percept of a fearful or happy face in
119 trials where a neutral face is presented (i.e., False Alarm, FA trials) cannot be explained by sensory input
120 of the presented face but is instead likely caused by anticipatory top-down processing. Although it is
121 expected that participants' anticipation for an upcoming threat-relevant fearful face target is noisy and
122 fluctuates similarly across all trials, the proportion of trials where a higher level of anticipation contributes
123 to the percept of a fearful face is likely to be larger among the FA than the HIT trials (**Fig. 1-1**).

124 We used ultra-high-field 7T fMRI with a spatial resolution of 0.8 mm to assess the activity of the
125 pulvinar as well as V1 during the detection tasks. Such high spatial resolution enabled us to infer the
126 cortical-depth dependent activity of V1 (Norris and Polimeni, 2019). The cortical-depth measurement is
127 advantageous because the activity related to threat anticipation may be particularly observed in V1
128 superficial cortical depth, where non-sensory driven activity has been observed (Muckli et al., 2015). We
129 predicted that the anticipation-driven false perception of a fearful face may be accompanied with
130 enhanced activity in the pulvinar and V1, as well as the potentially enhanced functional connectivity
131 between these two areas.

132

Materials and Methods

134

135 Participants

136 We enrolled 12 participants (6 males, mean age $23.73 \pm SD 3.64$, 2 left-handed), who provided written
137 consent and received monetary reward after the experiment. Participants were all healthy and had normal
138 or corrected-to-normal vision. The experiment protocol was approved by the ethical committee of

139 Maastricht University. The data of one participant were removed from analysis due to excessive head
140 motion (mean across runs > 4 mm).

141 We estimated that a sample size of $N = 11$ would be satisfactory to detect a medium to large
142 effect size ($f = .30$) with an alpha power of 0.05 and power of 80% (G*Power version 3.1.9.2) as
143 estimated with our 3T fMRI pilot results for pulvinar activity. Although we initially aimed for $N = 12$ to be
144 conservative, one participant was removed from analysis as described above, leaving us with $N = 11$.
145 Note that the sample size here is equivalent or larger than the related recent studies with 7T fMRI (e.g.,
146 four or 10 analyzed participants (Muckli et al., 2015; Kok et al., 2016).

147

148 **Stimuli**

149 Face images of 6 models (3 males) displaying fearful, happy, and neutral expressions were taken from
150 the NimStim face stimulus set (Tottenham et al., 2009). We only included face images with the mouth
151 open so that the local feature of an opened mouth alone would not enable detection of a fearful or happy
152 rather than a neutral face. The images were grey-scaled and cropped into oval shapes to eliminate hair.
153 They were then matched for luminosity, contrast, and spatial frequency spectrum with the SHINE toolbox
154 (Willenbockel et al., 2010) implemented in MATLAB (R2011b, The Mathworks, Natick, Massachusetts,
155 USA). We refrained from further manipulation of stimulus properties, as excessive manipulation itself
156 could unintentionally induce differential activity in V1, which is sensitive to lower-level stimulus properties.

157

158 **Experimental Design**

159 Participants completed 2 sessions, in which either fearful or happy face targets were presented in a
160 counterbalanced order.

161 The fearful face detection task required participants to detect a briefly presented fearful face
162 followed by a mask (neutral face) (Fig. 1). On each trial, either a fearful or neutral face appeared as a
163 target for 33 ms. Following a blank of 16.7 ms, a neutral face was presented for 133 ms as a mask that
164 rendered the target face less visible but did not completely abolish its visibility. The model for the mask
165 face was always different from the model for the target face. We used a neutral face as a mask instead of
166 simpler images such as checkerboards, because V1 typically shows preferential activity towards simpler

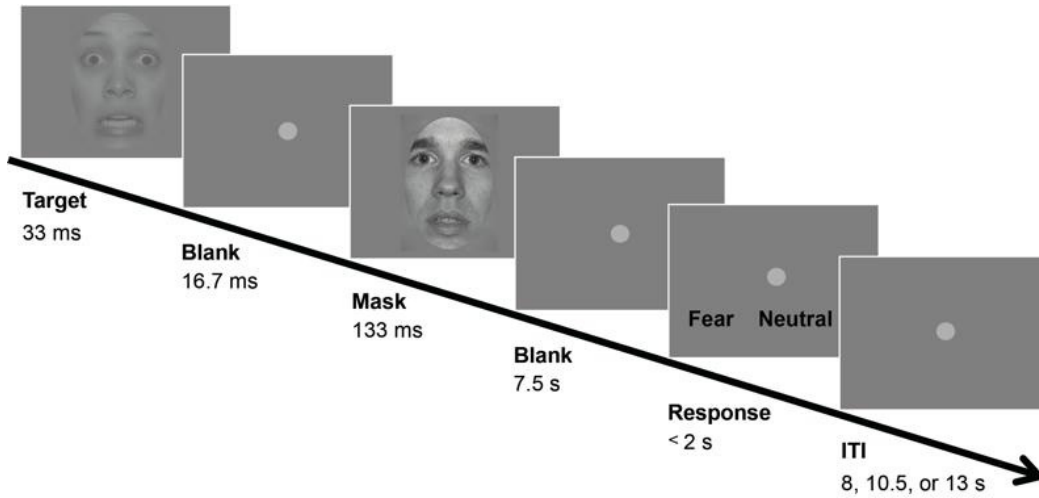
167 visual features (e.g., contrast and edges) and use of simple image masks could have interfered with the
168 measurement of the critical activity in V1 related to face processing.

169 To further control task difficulty, the contrast of the target face was reduced to 35% of the contrast
170 of the mask face, as determined during our pilot study. After 8.13 s after the target onset, response key
171 assignment was shown on the screen. A fearful or neutral face response was assigned randomly to either
172 the left or right key. Participants were instructed to respond with their right hand their first guess on
173 whether they had perceived a fearful or neutral face target within a 2s time window. After a jittered inter-
174 trial-interval from the onset of response assignment (8, 10.5, or 13 s), another trial was initiated. There
175 were 24 trials in each of 8 runs (8 min 10 s per run), comprising 12 trials each for fearful and neutral face
176 targets. There was no feedback provided on each trial. The order of trials was randomized.

177 In the control task session, we used happy faces, which are emotionally salient but non-
178 threatening. The task was otherwise identical to the fear condition and used the same neutral face stimuli.
179 The fearful and happy face sessions were conducted on two separate days in a counterbalanced order
180 across participants. Stimuli were presented with Psychtoolbox (Brainard, 1997) implemented in Matlab
181 (R2012a, the Mathworks).

182 For the data analysis the percept of participants was classified as follows: The correct percept of
183 the presented fearful or happy target face was classified as HIT, whereas the false percept of a fearful or
184 happy face in trials where a neutral face was presented was classified as FA. The correct percept of the
185 presented neutral face was classified as Correct Rejection (CR), whereas the incorrect percept of a
186 neutral face in trials where a fearful or happy face was presented was classified as MISS.

187



188

189 **Figure 1. Design of the fearful face detection task.** In each trial, either a fearful face target or a neutral
 190 face was presented briefly, followed by a mask consisting of a neutral face with a different identity than
 191 the target face. Participants responded whether they perceived a fearful target or neutral face by pressing
 192 the response key, which was randomly assigned trial-wise. The control task used happy face targets and
 193 neutral faces (not shown), and otherwise identical procedures. ITI: inter-trial interval. See also **Fig. 1-1.**

194

195 **fMRI data acquisition**

196 MRI data were acquired with a 7T Magnetom scanner (Siemens, Erlangen, Germany) at the Scannexus
 197 facility located at the Department of Cognitive Neuroscience, Faculty of Psychology and Neurosciences,
 198 Maastricht University (NL), with a Nova 1-transmitter/32-receiver head coil (Nova Medical, Wilmington,
 199 USA). For functional data acquisition, 2D gradient-echo planar images (EPI) were acquired at 0.8 mm
 200 isotropic resolution, with the following parameters: repetition time (TR) = 2500 ms, echo time (TE) = 21.8
 201 ms, flip angle = 80, GRAPPA acceleration factor = 3, matrix size = 154 × 236, field of view (FOV) = 123
 202 mm × 188 mm, slice thickness = 0.8 mm, number of slices = 40, no gaps, echo spacing = 1.04 ms,
 203 Bandwidth = 1116 Hz/Px, no multi-band acceleration. The slices were oriented to cover both the pulvinar
 204 and V1. To achieve maximal brain coverage with these parameters, right to left (RL) phase encoding was
 205 used for the task runs, so that the temporal areas outside the FOV were folded within the FOV and were
 206 trimmed later offline. A run of 5 TRs with the same parameters but with the opposing left to right (LR)

207 phase encoding direction was acquired immediately before each task run for offline top-up EPI distortion
208 correction (see *fMRI processing* for more details).

209 A separate run (3 min 30 s) was acquired to define V1 (see *Retinotopic delineation of V1*).

210 For anatomical data in 9 participants, a T1-weighted scan and a proton-density-weighted scan
211 were acquired with a resolution of 0.6 mm isotropic (FOV = 229 mm × 229 mm, matrix size = 384 × 384,
212 flip angle = 5. T1-weighted: TR = 3100 ms, TE = 2.52 ms; proton-density-weighted: TR = 1440 ms, TE =
213 2.52 ms). For the other 3 participants, we used anatomical images with a spatial resolution of 0.7 mm
214 isotropic from previous unrelated experiments.

215

216 **fMRI processing**

217 fMRI analyses were conducted in BrainVoyager 20.2 (Brain Innovation, Maastricht, the Netherlands). For
218 preprocessing of fMRI data, we trimmed the lateral sides of EPI images by a small amount (60 voxels) to
219 remove the folded-in tissue outside the FOV. The folding-in and trimming did not affect the coverage of
220 the bilateral pulvinar and V1. The trimmed EPI images were then slice time corrected (sinc interpolation)
221 and corrected for 3D rigid body motion (trilinear/sinc interpolation). Distortions of the EPI images from the
222 task runs were adjusted against EPI images taken immediately before each task run with the opposing
223 encoding phase (Andersson et al., 2003), with the BrainVoyager plugin COPE
224 (<http://support.brainvoyager.com/available-tools/49-available-plugins/477-cope-plugin-for-epi-distortion-correction.html>). EPI images then underwent temporal high-pass filtering with 2 cycles per run. That is,
225 signals with temporal frequency lower than half the length of a run (i.e., 250 s) were removed with
226 discrete Fourier filter.

227 After the preprocessing EPI images were manually aligned to the anatomical images in
228 BrainVoyager including optimization of alignment around the posterior portion of the brain encompassing
229 V1 and the pulvinar. From the total of runs those with 3D motion larger than 2.5 mm were discarded from
230 analyses, because large motion induced excessive and/or unique EPI distortion that interfered with
231 precise alignment and the subsequent cortical depth specific analyses. One participant's data were
232 excluded from further analysis due to excessive head movements (> 4 mm). For the remaining
233 participants, the run numbers included in analyses did not differ between the fearful face task ($M = 7.64 \pm$

235 SD 0.67) and the happy face task ($M = 7.45 \pm 0.82$) ($t(10) = 0.482$, $p = 0.640$). The mean numbers of
236 trials entered into the fMRI analyses for each participant, after excluding runs with excessive head motion
237 were: fearful HIT, $M = 45.64 \pm$ s.e. 4.0; fearful FA, 26.64 ± 3.48 ; happy HIT, 54.18 ± 4.32 ; happy FA,
238 21.18 ± 2.93 .

239 Task-related activity was then estimated with a deconvolution analysis, in which responses for
240 successive 5 points (2.5 s \times 5 TRs) were estimated for each of the 8 conditions, starting from the onset of
241 the target face for each of the 8 experimental conditions (fearful face HIT, MISS, FA, CR, as well as
242 happy face HIT, MISS, FA, CR). We used the deconvolution analysis because it does not assume a fixed
243 haemodynamic response function, which is generally built based on the response properties in sensory
244 cortical areas (Boynton et al., 1996; Glover, 1999) and is thus potentially less favorable for thalamic
245 areas. The entire deconvolved time course in V1 and the pulvinar are shown in **Fig. 2-1**. Additionally, the
246 GLM model included 6 head-motion nuisance parameters (3 translation directions and 3 rotation axes).
247 EPs were spatially smoothed only when localizing the task-relevant voxels but were not smoothed when
248 estimating the task-related activity to maintain laminar specificity.

249

250 **Localization of the pulvinar and LGN**

251 We localized the pulvinar as the target region, as well as the LGN as a control region (**Fig. 2**). Each of the
252 thalamic regions (the pulvinar and LGN) was first anatomically defined based on their physical properties.
253 Specifically, the pulvinar was located in the dorsal thalamus that is superior and medial to the LGN,
254 located adjacent to the third ventricle (Kastner et al., 2004; Sprenger et al., 2012; Mai, 2015). To localize
255 the pulvinar, we referred to the histological atlas (Chakravarty et al., 2006) superimposed on the high-
256 resolution T1 resampled at 0.8 mm in native space. In order to specifically select task-relevant voxels
257 within the anatomically localized pulvinar, functional images from the task runs were smoothed with a
258 gaussian kernel of 2.4 mm full width at half maximum (FWHM). Task-relevant voxels were then defined
259 based on activation at the temporal peak of the time course (5 s from the target face onset while
260 considering a haemodynamic delay of 5 s, i.e., 2 TRs \times 2.5 s) that was larger than baseline at a threshold
261 of $p < 0.01$ uncorrected to compensate for a generally lower tSNR in subcortical areas (see *Estimation of*

262 *tSNRs*). Note that task-relevant voxels were selected based on the target face onsets from all trials
263 including all conditions, to minimize any bias towards one particular condition over another.

264 Pulvinar ROIs were located in both hemispheres for all participants except for 1 participant (ROI
265 in the left hemisphere only). LGN ROIs were located in both hemispheres for 5 participants, while they
266 were located in either the right or left hemisphere for 4 and 2 participants, respectively. Inability to locate
267 the ROIs in both hemispheres in some participants is likely to be due to the generally hindered SNR
268 towards deeper brain areas (see *Estimation of tSNRs*). For participants with pulvinar and/or LGN ROI(s)
269 located in both hemispheres, activity was estimated for each hemisphere and averaged.

270

271 **Retinotopic delineation of V1**

272 To delineate V1 in each participant, a retinotopy run was acquired. During the run, color/luminance-
273 flickering wedge-shaped checkerboard patterns (30 deg in polar angle) were presented along the
274 horizontal or vertical meridian alternately for 15 s, each with 6 repetitions, following procedure in (Lafer-
275 Sousa and Conway, 2013). Checkerboard patterns were flickered at 4 Hz and were displayed in 1 of 4
276 color combinations (red/green, blue/yellow, black/white, and magenta/cyan) to activate neurons with
277 various response profiles and enhance the signals to identify the boundaries between the cortical areas.
278 The boundaries of V1 were delineated with a general linear model contrasting activity between the
279 horizontal and vertical presentation periods as previously described (Lafer-Sousa and Conway, 2013).
280 V2, V3, and V4 were delineated in a similar manner and served as control regions. The boundary of V4
281 was located while additionally referring to its predefined anatomical landmarks (Witthoft et al., 2014).

282

283 **Anatomical image processing and cortical-depth specific estimation of V1 activity**

284 Inhomogeneity of T1-weighted images was corrected by dividing the original image intensities by the
285 proton density images (Van de Moortele et al., 2009). Subsequently, the corrected T1 image was
286 resampled at a resolution of 0.8 mm to match the resolution of EPI. The boundaries of grey-white matter
287 and the pial surface were first estimated with BrainVoyager 20.2, and further corrected manually, to
288 improve the precision and to remove the blood vessels and dura mater based on image intensity. The

289 anatomical image was not transformed to standardized coordinates but was kept in native space, to
290 reduce resampling and maintain its laminar properties undistorted.

291 As was done for the pulvinar, the task-relevant voxels were selected within the delineated V1 of
292 each hemisphere. Specifically, the task-relevant voxels were defined based on the contrast between all
293 target face onsets versus baseline at a threshold of $p < 0.001$ uncorrected, at the temporal peak of the
294 time course at 5 s (2 TRs \times 2.5 s). The task-relevant voxels within V1 were successfully located in both
295 hemispheres in 8 participants, while they were located in only one hemisphere in the remaining 3
296 participants (right only, N = 1; left only, N = 2). For participants with peaks located in both hemispheres,
297 the estimates of activity were averaged between the hemispheres for each visual cortical area (e.g., V1).

298 To define the cortical depths of V1, we used the Laplace equation to estimate cortical thickness
299 and then obtained an equidistant definition of depth with respect to the local thickness (Muckli et al.,
300 2015; De Martino et al., 2018) at three depth levels (from 25, 50, and 75% depth levels relative to the
301 local cortical depth in an inward direction) centering around the spatial activity peak (i.e., voxel with
302 highest activation level) among the pre-defined task-relevant voxels with 15 \times 15 grids of 0.5 voxels.
303 Individual voxels were assigned to the adjacent cortical depth, and were used as regions of interest
304 (ROIs) in the subsequent analyses (**Fig. 3**). We confined our analyses to voxels allocated to the
305 superficial and deep cortical depth groups, which roughly correspond to cortical layers 1 to 3 and layers 5
306 to 6, respectively, due to the difference in anatomical thickness of each layer (de Sousa et al., 2010; Kok
307 et al., 2016). The voxels assigned to the superficial and deep depths covered an average of 22.67% (s.e.
308 = 3.95) of the retinotopically delineated V1 (see *V1 delineation*). This relatively small coverage by the
309 task-relevant voxels is likely to be due to lower contrast and luminosity as well as smaller stimulus size
310 relative to the V1 delineation run (i.e., The visual angles spanned by the checkerboards wedges and the
311 task face images were 10.4° \times 10.4° and 6.1° \times 4.5°, respectively). The cortical-depth dependent activity
312 was estimated from the unsmoothed functional data in order to maintain the original spatial resolution
313 (0.8mm).

314 We localized the control areas V2-4 in a similar manner as V1. The task-relevant voxels within V2
315 and V3 were successfully located in both hemispheres in 9 participants, while they were localized in only
316 one hemisphere in 2 participants (V2 right only, N = 1; V2 left only, N = 1; V3 right only, N = 1; V3 left

317 only, $N = 1$). The cortical depths of V2 and V3 were defined separately for the dorsal and ventral areas,
318 and the voxels for each cortical depth were combined between the dorsal and ventral areas. The task-
319 relevant voxels within V4 were located in both hemispheres in all participants.

320
321 **Estimation of tSNRs**
322 The SNR of the time series (tSNRs) for the pulvinar, LGN, and V1 superficial and deep cortical depths
323 were assessed with VTC inspector plugin in BrainVoyager (Brain Innovation). tSNR was assessed for
324 each ROI from the time course in initial runs of the tasks and averaged across participants. The mean
325 tSNR (\pm s.d.) was 8.12 (\pm 1.03) for the pulvinar, 7.06 (\pm 1.38) for LGN, 18.15 (\pm 4.48) for V1 superficial
326 cortical depth and 18.04 (\pm 3.92) for V1 deep cortical depth. In line with the previous report that the
327 gradient-echo imaging sequence employed here yields higher SNR towards the surface of the cortex (De
328 Martino et al., 2018), thalamic areas (i.e., the pulvinar and LGN) that were deeper inside the brain and
329 further from the coil had lower tSNR relative to V1 on the outer brain.

330
331 **Generalized form of context-dependent psychophysiological interaction analysis (gPPI)**
332 To examine whether functional connectivity between the pulvinar and V1 was enhanced during certain
333 trial types (e.g., FA trials with fearful faces), we conducted a pair of gPPI analyses (McLaren et al., 2012):
334 one with V1 superficial cortical depth voxels as the seed ROI, and the other with V1 deep cortical depth
335 voxels as the seed ROI. For each analysis, the GLM model included regressors for each of the eight trial
336 types (i.e., HIT, FA, MISS, CR for fearful and happy faces) convolved with the canonical two-gamma
337 HRF, a regressor for the z-normalized time course of the seed ROI, regressors for PPI terms (i.e., seed
338 time course \times trial type regressor), six nuisance regressors of 3D head motion (3 translation directions
339 and 3 rotation axes). The GLM analysis was run for each participant, and the parameter estimates (Beta
340 values) were extracted within the pulvinar ROI (see *Materials and Methods* for ROI definition) for the PPI
341 term of HIT and FA trials of fearful and happy faces (i.e., the four critical trial types included in the main
342 results). In the group-level analysis, t-values for the parameter estimates for each trial type and seed ROI
343 in gPPI (**Fig. 3-2**) were tested against 0 with a one-sample t-test, with Bonferroni correction for eight
344 conditions (i.e., $p = 0.05/8$, HIT/FA \times Fearful/Happy \times V1 superficial/deep cortical depths).

345

346

347 **Statistical Analysis**

348 We conducted subject-level analyses of fMRI data in BrainVoyager 20.2 (Brain Innovation, Maastricht,
349 The Netherlands) (see *fMRI processing*), and subsequently, conducted group-level repeated measures
350 ANOVAs in IBM SPSS Statistics (version 18). The assumption of sphericity was met in the current
351 dataset because there were only two levels per factor (e.g., emotion) in each repeated ANOVA.
352 Behavioural performance was also analyzed in IBM SPSS.

353 Following previous studies (Keselman and Keselman, 1993; Tamaki et al., 2016), when an
354 omnibus 3-way repeated measures ANOVA revealed a significant 3-way interaction, we conducted 2-way
355 (n-1 way) repeated measures ANOVAs to locate a simple interaction effect. A significant 2-way interaction
356 that was identified was subsequently tested with a t-test (two-tailed) to examine simple main effects.
357 Similarly, when an omnibus repeated measures ANOVA initially involved only two factors (i.e., 2-way), a
358 significant interaction was similarly followed by t-tests (two-tailed). The series of t-tests were not
359 susceptible to the inflation of type 1 error as they followed significant interactions in the initial omnibus
360 ANOVAs, as has been validated and commonly practiced previously (Keselman and Keselman, 1993;
361 Cohen, 2004). We estimated effect sizes in the post-hoc t-tests with Cohen's d, where a value larger than
362 0.8 indicated a large effect size and a value larger than 0.5 indicated a medium effect size (Cohen, 1988;
363 Tamaki et al., 2016). All t-tests reported in this manuscript were two-tailed.

364

Results365 **Behavioural performance**

366 Perception of a fearful face reported on presentation of a fearful face target was classified as HIT,
367 whereas perception of a fearful face reported on presentation of a neutral face was classified as a false
368 alarm (FA) and similarly for the happy vs. neutral faces in the control task. The ratio of FA was similar
369 between the fearful face and the happy face detection task ($M = 28.51 \pm 3.52\%$; $M = 24.13 \pm 3.07\%$,
370 respectively), and the rates in each task did not significantly differ from each other ($t(10) = 1.845, p =$
371 0.095^a). The ratio of HIT trials was higher for the happy face ($M = 60.36 \pm \text{s.e. } 4.36\%$) than for the fearful
372 face detection task ($M = 49.18 \pm 4.42\%$) ($t(10) = -4.155, p = 0.002^b$). This is consistent with previous
373 literature showing that explicit labelling of happy faces is easier than that of negative faces (Calvo and
374 Lundqvist, 2008). Our choice of facial images with open mouth may have additionally contributed to
375 relatively poorer detection of a fearful face against a neutral face target or mask because a neutral face
376 may look more similar to a fearful face with opened mouth.

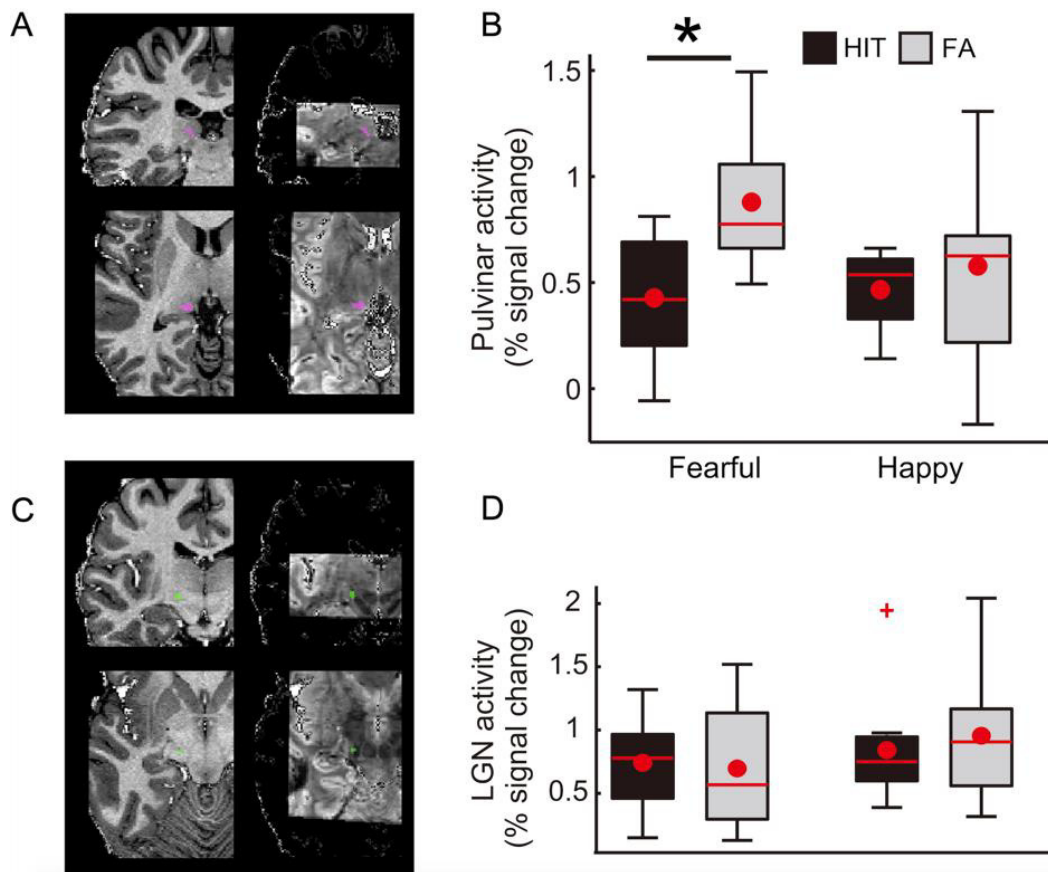
377

378 **Pulvinar activity during the detection tasks**

379 Our primary interest was how activity of the higher-order thalamic area pulvinar (**Fig. 2A**) may differ
380 between HIT and FA trials, and whether such a difference is specific to the fearful face detection task.

381 We observed that pulvinar activity was greater on FA trials than on HIT trials (**Fig. 2B**), as
382 demonstrated by a main effect of percept type in a repeated measures ANOVA ($F(1,10) = 8.310, p =$
383 0.016). Greater activity in FA trials relative to HIT trials was observed during the fearful face detection
384 task ($t(10) = -2.944, p = 0.015, d = 0.8^c$) but not during the happy face detection task ($t(10) = -1.23, p =$
385 $0.247, \text{n.s.}^d$). There was no significant difference between FA trials of the fearful face detection task and
386 that of the happy face detection tasks ($t(10) = .572, p = .580, \text{n.s.}^e$). There was no significant interaction
387 between percept type and emotion ($F(1,10) = 0.155, p = 0.702$). The main effect of percept type
388 independent of emotion suggests that the pulvinar shows enhanced activity with a false percept in
389 general, as has been reported in a previous study during a false detection of change in non-emotional
390 stimuli (Pessoa and Ungerleider, 2004) (see also **Fig. 2-1** for the deconvolved time course of the
391 pulvinar).

392 As a control analysis for the pulvinar activity, we examined the activity of a first-order thalamic
 393 region, the LGN (Fig. 2C). Our analysis showed that the activity level of the LGN was not altered in FA
 394 trials of fearful faces (Fig. 2D). Neither the main effect of percept type nor that of emotion was significant
 395 in a repeated-measures ANOVA ($F(1,10) = 0.100, p = 0.759; F(1,10) = 3.014, p = 0.113$, respectively^f).
 396 The two-way interaction was also non-significant ($F(1,10) = 0.363, p = 0.560$). The result of this control
 397 analysis suggests the pulvinar, rather than the thalamic areas in general, contributed to FA trials.
 398



399
 400 **Figure 2. Activity in the pulvinar and LGN.** **A.** Demonstrations of pulvinar ROIs from a representative
 401 participant (see *Materials and Methods* for ROI definition), shown on the anatomical image (left panels)
 402 and EPI (right panels). **B.** Pulvinar showed enhanced activity in FA trials relative to HIT trials during the
 403 fearful face detection task ($t(10) = -2.944, p = 0.015, d = 0.8$) but not during the happy face detection task

404 ($t(10) = -1.23, p = 0.247$, n.s.). There was no significant interaction between percept type and emotion
405 ($F(1,10) = 0.155, p = 0.702$). Here, data from one participant with an extreme outlier (activity exceeding 5
406 standard deviations above the group mean across four conditions, i.e., HIT/FA x fearful/happy) are not
407 shown. **C.** Demonstrations of the LGN ROI from an example participant (see *Materials and Methods* for
408 ROI definition). **D.** Unlike the pulvinar, the LGN showed no differential activity between the percept types
409 and facial emotions. Box plot shows upper (75%) and lower (25%) quartiles with median (red line) and
410 mean (red dot), with whisker showing maximum and minimum value. An outlier (outside of ± 2.7 standard
411 deviations within a distribution for a given condition) is shown with a red cross. * $p < 0.05$. See also **Fig. 2-**
412 **1 and 2-2.**

413

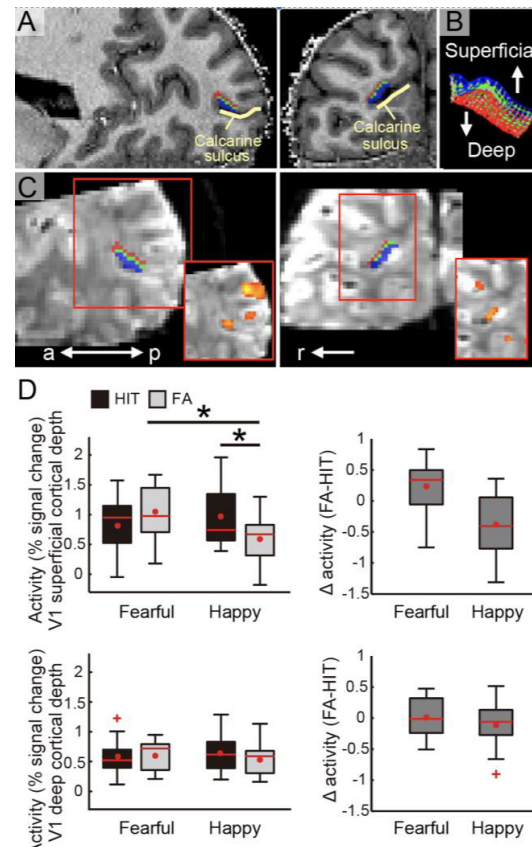
414 **Cortical-depth dependent V1 activity during fearful face perception**

415 While pulvinar activity alone did not dissociate between fearful and happy faces (**Fig. 2**), we observed
416 that V1 superficial activity did (**Fig. 3D**). A repeated measures analysis of variance (ANOVA) revealed a
417 second-order interaction between percept type (HIT/FA), emotion (fearful/happy), and cortical depth
418 (superficial深深) of V1 ($F(1,10) = 5.667, p = 0.039$). This interaction was due to the fact that percept type
419 and emotion interactively modulated V1 activity at superficial cortical depths ($F(1, 10) = 7.840, p = .019$),
420 but not at deep cortical depths ($F(1,10) = 0.673, p = .431$) (see **Fig. 2-1** for the deconvolved V1 time
421 course and **Fig. 3-1** for the results separately plotted for individual participants).

422 At the superficial depth, V1 activity in FA trials of a happy face was less than that in HIT trials of a
423 happy face ($t(10) = 2.387, p = 0.038, d = 0.9^g$). This result is consistent with a previous study
424 demonstrating that V1 activity levels are typically greater for HIT than for FA trials in a visual detection
425 task with non-threatening targets (Ress and Heeger, 2003), although cortical depth dependent activities
426 were not reported.

427 Contrary to the happy face detection task, V1 superficial depth activity in FA trials during the
428 fearful face detection task was similar to or even numerically larger than that in HIT trials ($t(10) = -1.714, p$
429 $= 0.117$, n.s.^h). Indeed, post-hoc analysis showed that V1 superficial depth activity in FA trials of a fearful
430 face was significantly greater than that in FA trials of a happy face ($t(10) = -2.486, p = 0.032, d = 0.8^i$),
431 even though the same neutral faces were presented with the only difference being the task context to

432 anticipate either a fearful or happy face target. These results are consistent with the idea that anticipation-
 433 driven activity, which is more evident in the FA trials than in the HIT trials, was added on top of the
 434 smaller input-driven activity in FA trials. In other words, our results suggest that V1 superficial depth
 435 activity may reflect excessive top-down processing in anticipation of fearful face targets, which does not
 436 generalize to mere anticipation of any emotionally salient target (i.e., happy faces).



437
 438 **Figure 3. Demonstrations of V1 cortical depths and cortical-depth dependent activity during the**
 439 **tasks. A.** V1 cortical depth is visualized on an anatomical image of a representative participant with
 440 sagittal (left panel) and coronal views (right panel). The voxels allocated to superficial (outwards to pial
 441 surface) and deep (inwards to white matter) cortical depths are shown in blue and red, respectively. The
 442 voxels allocated to the intermediate depth (shown in green) were disregarded in the main analyses (see
 443 *Materials and Methods*). **B.** The cortical grid mesh within which the voxels were allocated. **C.** The V1

444 cortical depth is visualized on EPI images (visualized in 3D for demonstrative purpose) in sagittal and
445 coronal views (left and right, respectively). Red squares at the lower right demonstrate activity for all face
446 targets relative to baseline on the EPI smoothed with a 3D kernel of 2.4 mm full width at half maximum
447 (FWHM). **D.** Peak activity at V1 superficial and deep cortical depths (upper and lower rows, respectively)
448 in HIT and false alarm (FA) trials in the fearful face and happy face detection tasks. The difference in
449 activity between FA and HIT trials are demonstrated in the right panel for each task, with a larger value
450 indicating greater activity for FA than for HIT trials. Box plot shows upper (75%) and lower (25%) quartiles
451 with median (red line) and mean (red dot), with whisker showing maximum and minimum value. An outlier
452 (outside of ± 2.7 standard deviations within a distribution for a given condition) is shown with a red cross.
453 a: anterior, p: posterior, r: right, * $p < 0.05$. See also **Fig. 2-1, 3-1, 3-2, 3-3, 3-4**.

454

455 **Connectivity between the pulvinar and V1 during fearful face perception**

456 The aforementioned results showed that V1 superficial depth activity in FA trials was enhanced only for
457 fearful faces and pulvinar activity was higher in FA trials than in HIT trials regardless of face type. Given
458 that there is a reciprocal interaction between the pulvinar and V1 including modulatory input from the
459 pulvinar to V1 superficial layers (Shipp, 2003; Purushothaman et al., 2012; Cicmil and Krug, 2015; Bridge
460 et al., 2016; Roth et al., 2016; Shipp, 2016), it is possible that the enhanced V1 superficial depth activity
461 in FA trials of fearful faces is at least partly related to its communication with the pulvinar. We examined
462 whether a modulation of activity was present between the pulvinar, and the superficial or deep V1 voxels
463 using a generalized form of context-dependent psychophysiological interactions analysis (gPPI) (McLaren
464 et al., 2012). A functional coupling was present between the pulvinar and V1 superficial depth in FA trials
465 for fearful faces ($t(10) = 3.981$, $p = 0.0026$, one sample t-test against 0, CI [0.319 1.128]¹; **Fig. 3-2**), but
466 not in the other conditions tested (fearful HIT: $t(10) = 0.403$, $p = 0.695$, CI [-0.683 0.985]; happy HIT: $t(10)$
467 = 1.869, $p = 0.091$, CI [-0.105 1.120]; happy FA: $t(10) = 1.4364$, $p = 0.181$, CI [-0.271 1.253]). In addition,
468 another analysis hinted that there was already enhanced activity in the pulvinar prior to the onset of FA
469 trials with fearful faces but not in V1 superficial depth (**Fig. 3-3**). This result, together with the result of
470 gPPI analysis, suggests that the modulatory input from the pulvinar may have contributed to the
471 enhanced V1 superficial activity in FA trials with fearful face percept, although future studies need to

472 directly test the specific direction of interaction between the two regions. There was no significant
473 interaction with V1 cortical depth and facial emotions in the gPPI result ($F(1,10)=.198, p = .666$) (**Fig. 3-**
474 **2**).

475

476 **Control analyses**

477 To examine the specificity of our results, we conducted a series of control analyses. We particularly
478 examined the potential additional contributions of higher visual cortical areas, V2, V3, and V4 in the FA
479 trials for fearful faces. The activity of these areas was examined separately for their superficial and deep
480 cortical depths in a manner similarly to V1 (see **Fig. 4A** and *Materials and Methods*). Other higher visual
481 areas such as fusiform areas were outside of the fMRI coverage.

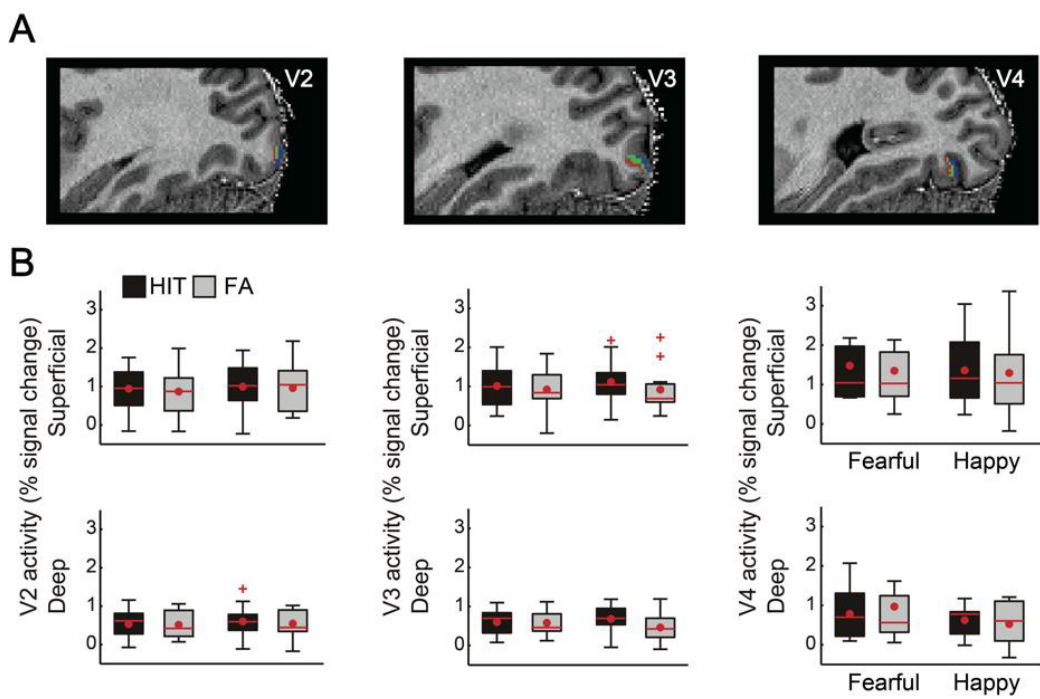
482 Unlike V1, we found that the activity of V2-V4 was not enhanced in the FA trials of fearful faces
483 (**Fig. 4B**). With V2, a second-order interaction between percept type, emotion, and cortical depth was
484 non-significant ($F(1,10) = 0.397, p = 0.543$). The main effects of percept type and emotion were also non-
485 significant ($F(1,10) = 0.612, p = 0.452; F(1,10) = 0.240, p = 0.635$, respectively), while only the main
486 effect of cortical depth was significant ($F(1,10) = 21.245, p = 0.001$). Similarly, with V3, a second-order
487 interaction was non-significant ($F(1,10) = 0.265, p = 0.618$). Although there was a general trend that the
488 activity on HIT trials was larger relative to FA trials, the main effect of percept type did not reach
489 significance ($F(1,10) = 4.534, p = 0.059$). The main effect of percept type was also non-significant
490 ($F(1,10) = 0.018, p = 0.895$), while a main effect of cortical depth was significant ($F(1,10) = 20.434, p =$
491 0.001). Likewise, with V4, a second-order interaction ($F(1,10) = 1.028, p = 0.335$) as well as the main
492 effects of percept type and emotion were non-significant ($F(1,10) = 0.124, p = 0.732; F(1,10) = 0.850, p =$
493 0.37 , respectively), while only the main effect of cortical depth was significant ($F(1,10) = 18.523, p =$
494 0.002).

495 As an additional control analysis, we examined whether similar results to those observed in FA
496 trials of fearful faces would be present in MISS trials, in which a fearful face was presented but not
497 detected. While the aforementioned results for FA trials of fearful faces may reflect enhanced top-down
498 processing as we speculated earlier, other non-mutually exclusive possibilities are worth considering.
499 Specifically, the results in FA trials may reflect a mere 'missing' of a presented face image, in which case

500 similar results as FA trials would be expected in MISS trials. Contrary to this possibility, we did not
 501 observe any notable results specific to MISS trials of fearful faces either in V1 or in the pulvinar (a non-
 502 significant interaction between percept type (MISS/CR) and emotion: $F(1,10) = 0.013, p = 0.912$) (**Fig. 3-4**), excluding the possibility that the results in FA trials of fearful faces merely reflected a mere missing of
 503 a presented face image yielding a mismatch between the input and percept.

504 Taken together, the analyses suggest that the results of pulvinar and V1 superficial cortical depth
 505 in false perception of fearful faces were not mirrored in the LGN or in V2-4. The findings also indicate that
 506 the results of pulvinar and V1 were not explained away either by mere anticipation of any emotionally
 507 salient target (i.e., happy face) or by mere mismatch between percept and input, suggesting the
 508 specificity of the involvement of pulvinar-to-V1 input in false perception of fearful faces.

510



511
 512 **Figure 4. Control analyses showing no differential activity in V2, V3, and V4 in HIT compared with**
 513 **false alarm (FA) trials. A.** V2, V3, and V4 cortical depths are visualized on the anatomical image of an
 514 example participant, with the same color coding as for V1 shown in **Fig. 3** (see *Materials and Methods* for

515 ROI definition). **B.** Unlike V1, V2-4 did not show any differential activity between the percept types and
516 facial emotions, regardless of cortical depth. Box plot shows upper (75%) and lower (25%) quartiles with
517 median (red line) and mean (red dot), with whisker showing maximum and minimum value. An outlier
518 (outside of ± 2.7 standard deviations within a distribution for a given condition) is shown with a red cross.
519
520

521

Statistical Table

Data structure	Type of test	Confidence Interval
a Normal distribution	Paired-sample t-test (two-tailed)	[-0.173 -0.052]
b Normal distribution	Paired-sample t-test (two-tailed)	[-0.009 0.097]
c Normal distribution	Post-hoc t-test following ANOVA (two-tailed)	[-0.782 -0.108]
d Normal distribution	Post-hoc t-test following ANOVA (two-tailed)	[-0.888 0.256]
e Normal distribution	Post-hoc t-test following ANOVA (two-tailed)	[-0.391 0.661]
f Normal distribution	Post-hoc t-test following ANOVA (two-tailed)	fearful [-0.335 0.424]; happy [-0.500 .272]
g Normal distribution	Post-hoc t-test following ANOVA (two-tailed)	[0.025 0.735]
h Normal distribution	Post-hoc t-test following ANOVA (two-tailed)	[-0.542 0.071]
i Normal distribution	Post-hoc t-test following ANOVA (two-tailed)	[-0.871 -0.048]
j Normal distribution	One sample t-test (two-tailed)	[0.319 1.128]

522

523

Discussion

524 We observed that the false percept of anticipated but not present fearful face relative to that of a happy
 525 face was accompanied by increased activity in superficial cortical depth of V1, which constitutes the
 526 earliest stage of the visual cortical hierarchy. This enhanced V1 activity may particularly contribute to the
 527 anticipatory perception of threat signals, as it did not generalize to the perception of non-threatening
 528 signals, i.e., happy faces. Although preliminary, we additionally observed that the connectivity between
 529 the pulvinar and V1 superficial cortical depth was enhanced when participants falsely perceived fearful
 530 faces. These results suggest a potential role of the pulvinar and V1 in preparing the visual system to
 531 perceive an anticipated threat.

532 It may be counterintuitive to expect a crucial role of V1 in the perception of fearful faces, given
 533 that V1 is fine-tuned to low-level visual features that would constitute only low-level properties of fearful
 534 faces. Nevertheless, recent findings suggest that a lower visual cortical area can reflect higher-level
 535 features, when the prediction signals for such features originate from a higher area (Schwiedrzik and
 536 Freiwald, 2017). While such top-down signals are typically expected to descend from higher cortical
 537 areas, it has recently been speculated that the pulvinar also contributes to such top-down signals (Kanai
 538 et al., 2015), including contextual signals (Roth et al., 2016). Given that the pulvinar appears capable of

539 coding threat signals, including a complex fearful face (de Gelder, 2006; Pessoa and Adolphs, 2010), one
540 possibility is that the pulvinar serves as one of the critical regions to modulate the early stage processing
541 in V1 rapidly biasing visual cortical processing towards threat perception.

542 In line with this, a recent MEG study with human participants demonstrated that the neural activity
543 driven by the inputs of facial images is better explained by a dynamic causal model which considers the
544 pulvinar-to-V1 input, and that such input is modulated by the presence of fearful expression in faces
545 (McFadyen et al., 2017). While this study suggests the role of the pulvinar in input-driven relaying of
546 information to V1, our study suggests that the pulvinar may play an additional role in modulating activity in
547 the early stage of visual cortex in anticipation of threat-relevant signals in humans.

548 Limitations of the current study do not allow a more direct conclusion of the direction of the
549 interaction. First, the temporal resolution of fMRI was not high enough to detect the precedence of one
550 region over the other, which may be compensated for in a future study using MEG with higher temporal
551 resolution. Secondly, the portions of the pulvinar active for the FA of fearful faces were not always
552 symmetrical between the hemispheres and did not always converge to the anatomical subregions that
553 have direct communication with V1 (Bridge et al., 2016) (Figure 2-2). As the localization of the subregions
554 of the pulvinar may be partly precluded because of relatively lower SNR (see *Estimation of tSNRs*), future
555 studies may adopt alternative fMRI sequences for a better signal in the pulvinar. Future studies may also
556 examine whether the current results generalize when facial images and masks were controlled differently
557 (e.g., faces with closed mouth and non-facial masks).

558 The absence of enhanced V2-V4 activity in the FA trials of fearful faces may be surprising
559 considering that the pulvinar and V1 could both drive V2 activity (Marion et al., 2013). However, this null
560 result does not necessarily indicate that the enhanced activity in the pulvinar and/or V1 have no
561 subsequent effect in higher visual areas V2-V4 in the FA trials of fearful faces. This is because the input-
562 driven activity in V2-V4 is supposedly higher in HIT trials relative to FA trials (Ress and Heeger, 2003),
563 especially due to salient sensory inputs of the fearful face targets. Thus, the absence of activity difference
564 between the FA trials and HIT trials in these downstream areas of V1 may instead suggest that the
565 anticipation-driven activity in the pulvinar and/or V1 may have compensated the originally lower activity in
566 V2-V4 in the FA trials of fearful faces, making such activity comparable to the HIT trials of fearful faces.

567 Note that these null results do not exclude that other areas besides the pulvinar and V1 were involved in
568 false percept (i.e., FA trials) of fearful faces. Future studies should investigate whether and how the
569 pulvinar and V1 may interact with other areas, such as the amygdala, fusiform face area and prefrontal
570 areas not covered in this study. Whole brain analyses, which may help address such questions, were not
571 performed because of the restricted brain coverage (see *fMRI Data acquisition* in *Materials and Methods*),
572 and because the spatial distortion and/or SNR were expected to be highly inhomogeneous even across
573 the covered brain areas due to ultra-high magnetic field (see *Estimation of tSNRs*).

574 How false perception of non-threatening cues, such as happy faces, emerges remains to be
575 investigated. One possibility is that such a percept would reflect top-down modulation of visual cortical
576 areas higher than V1, similarly to the processing of facial identity (Schwiedrzik and Freiwald, 2017).
577 Although the control analyses did not support the contribution of V2-4 to the false perception of happy
578 face targets, one possibility may be that visual areas higher than V4 contributed here, although these
579 higher areas were not covered in this study (to allow for the spatial resolution desired).

580 How the subjective experience of falsely perceiving an unpresented fearful face may have
581 differed from that of correctly perceiving a presented fearful face is one remaining interesting question.
582 One way to examine the potential difference could be to assess perceptual confidence. Another way
583 could be to measure the whole brain activity to examine whether other brain areas, e.g., motor areas as
584 well as the pulvinar also implicated in action (Dominguez-Vargas et al., 2017), may have also contributed
585 to bias responses in false perception, although it is noteworthy that response bias could be explained by
586 the perceptual processing itself (Rahnev et al., 2011).

587 One potential limitation of the current method to estimate the cortical depth dependent activity is
588 that the gradient-echo imaging sequence employed here is known to have a better SNR towards the
589 surface of the cortex (De Martino et al., 2018). This SNR difference may mean that the study was
590 underpowered to elucidate potential additional contributions of V1 at the deep cortical depth, although a
591 previous study with similar 7T fMRI parameters has successfully elucidated significant effects in V1 even
592 at its deep cortical depths (Kok et al., 2016). The current results certainly suggest the involvement of V1
593 in the anticipatory processing of threat, but its layer-specificity may be further investigated in future
594 studies with fMRI sequences rather than gradient-echo.

595 The notion that the pulvinar plays a role in top-down modulation of fearful face processing is not
596 mutually exclusive with the traditional view emphasizing the role of the pulvinar in the subcortical route
597 ("low road") to process the presented threat signals in an input-driven manner. The subcortical route is
598 thought to bypass the cortex to rapidly relay the retinal input to the amygdala via the superior colliculus
599 and pulvinar (LeDoux, 1996; de Gelder, 2006). Such coarse input-driven processing has been speculated
600 to result in erroneous, false perception of threat signals (LeDoux, 1996). Although the function of such a
601 subcortical route may be relatively degraded in humans compared with other species such as rodents
602 (Pessoa and Adolphs, 2010; Bridge et al., 2016), its contribution has been demonstrated in humans
603 (Tamietto and de Gelder, 2010; Tamietto et al., 2012; Mendez-Bertolo et al., 2016).

604 Overall, the current results suggest that anticipatory processing of threat signals is distinct from
605 the input-driven processing of threat signals, with the former uniquely involving the engagement of the
606 pulvinar and V1 which constitute the earliest stage of visual processing hierarchy. Such anticipatory
607 processing of threat may contribute to the perception of threat-relevant images in the absence of
608 corresponding sensory inputs as in clinical cases of flashbacks reported in PTSD.

609

610 **Declaration of interest**

611 We declare no conflict of interest.

612

613

614

References

615

- 616 Andersson JL, Skare S, Ashburner J (2003) How to correct susceptibility distortions in spin-echo
617 echo-planar images: application to diffusion tensor imaging. *Neuroimage* 20:870-888.
- 618 Bishop SJ (2007) Neurocognitive mechanisms of anxiety: an integrative account. *Trends Cogn
619 Sci* 11:307-316.
- 620 Boynton GM, Engel SA, Glover GH, Heeger DJ (1996) Linear systems analysis of functional
621 magnetic resonance imaging in human V1. *J Neurosci* 16:4207-4221.
- 622 Brainard DH (1997) The Psychophysics Toolbox. *Spat Vis* 10:433-436.
- 623 Bridge H, Leopold DA, Bourne JA (2016) Adaptive Pulvinar Circuitry Supports Visual Cognition.
624 *Trends Cogn Sci* 20:146-157.
- 625 Calvo MG, Lundqvist D (2008) Facial expressions of emotion (KDEF): identification under
626 different display-duration conditions. *Behav Res Methods* 40:109-115.
- 627 Chakravarty MM, Bertrand G, Hodge CP, Sadikot AF, Collins DL (2006) The creation of a brain
628 atlas for image guided neurosurgery using serial histological data. *Neuroimage* 30:359-
629 376.
- 630 Cicmil N, Krug K (2015) Playing the electric light orchestra--how electrical stimulation of visual
631 cortex elucidates the neural basis of perception. *Philos Trans R Soc Lond B Biol Sci*
632 370:20140206.
- 633 Cohen BH (2004) Explaining Psychological Statistics. New York: John Wiley & Sons.
- 634 Cohen J (1988) Statistical Power Analysis for the Behavioral Sciences. Hillsdale: Lawrence
635 Erlbaum and Associates.
- 636 de Gelder B (2006) Towards the neurobiology of emotional body language. *Nat Rev Neurosci*
637 7:242-249.
- 638 De Martino F, Yacoub E, Kemper V, Moerel M, Uludag K, De Weerd P, Ugurbil K, Goebel R,
639 Formisano E (2018) The impact of ultra-high field MRI on cognitive and computational
640 neuroimaging. *Neuroimage* 168:366-382.
- 641 de Sousa AA, Sherwood CC, Schleicher A, Amunts K, MacLeod CE, Hof PR, Zilles K (2010)
642 Comparative cytoarchitectural analyses of striate and extrastriate areas in hominoids.
643 *Cereb Cortex* 20:966-981.
- 644 Dominguez-Vargas AU, Schneider L, Wilke M, Kagan I (2017) Electrical Microstimulation of the
645 Pulvinar Biases Saccade Choices and Reaction Times in a Time-Dependent Manner. *J
646 Neurosci* 37:2234-2257.
- 647 Friston K (2005) A theory of cortical responses. *Philos Trans R Soc Lond B Biol Sci* 360:815-
648 836.
- 649 Glover GH (1999) Deconvolution of impulse response in event-related BOLD fMRI. *Neuroimage*
650 9:416-429.
- 651 Grieve KL, Acuna C, Cudeiro J (2000) The primate pulvinar nuclei: vision and action. *Trends
652 Neurosci* 23:35-39.
- 653 Grillon C, O'Connell K, Lieberman L, Alvarez G, Geraci M, Pine DS, Ernst M (2017) Distinct
654 responses to predictable and unpredictable threat in anxiety pathologies: effect of panic
655 attack. *Biol Psychiatry Cogn Neuroimaging* 2:575-581.
- 656 Kanai R, Komura Y, Shipp S, Friston K (2015) Cerebral hierarchies: predictive processing,
657 precision and the pulvinar. *Philos Trans R Soc Lond B Biol Sci* 370.
- 658 Kastner S, O'Connor DH, Fukui MM, Fehd HM, Herwig U, Pinsk MA (2004) Functional imaging
659 of the human lateral geniculate nucleus and pulvinar. *J Neurophysiol* 91:438-448.
- 660 Keselman HJ, Keselman JC (1993) Analysis of repeated measurements. In: Applied Analysis of
661 Variance in Behavioral Science (Edwards LK, ed). New York.
- 662 Koizumi A, Mobbs D, Lau H (2016) Is fear perception special? Evidence at the level of decision-
663 making and subjective confidence. *Soc Cogn Affect Neurosci* 11:1772-1782.

- 664 Kok P, Bains LJ, van Mourik T, Norris DG, de Lange FP (2016) Selective Activation of the Deep
665 Layers of the Human Primary Visual Cortex by Top-Down Feedback. *Curr Biol* 26:371-
666 376.
- 667 Lafer-Sousa R, Conway BR (2013) Parallel, multi-stage processing of colors, faces and shapes
668 in macaque inferior temporal cortex. *Nat Neurosci* 16:1870-1878.
- 669 Lanzetta JT, Orr SP (1986) Excitatory strength of expressive faces: effects of happy and fear
670 expressions and context on the extinction of a conditioned fear response. *J Pers Soc
671 Psychol* 50:190-194.
- 672 LeDoux JE (1996) In: *The Emotional Brain* New York: Simon and Schuster.
- 673 Mai JKM, M.; & Paxinos, G. (2015) *Atlas of the Human Brain*.: Academic Press.
- 674 Marion R, Li K, Purushothaman G, Jiang Y, Casagrande VA (2013) Morphological and
675 neurochemical comparisons between pulvinar and V1 projections to V2. *J Comp Neurol*
676 521:813-832.
- 677 McFadyen J, Mermilliod M, Mattingley JB, Halasz V, Garrido MI (2017) A Rapid Subcortical
678 Amygdala Route for Faces Irrespective of Spatial Frequency and Emotion. *J Neurosci*
679 37:3864-3874.
- 680 McLaren DG, Ries ML, Xu G, Johnson SC (2012) A generalized form of context-dependent
681 psychophysiological interactions (gPPI): a comparison to standard approaches.
682 *Neuroimage* 61:1277-1286.
- 683 Mendez-Bertolo C, Moratti S, Toledano R, Lopez-Sosa F, Martinez-Alvarez R, Mah YH,
684 Vuilleumier P, Gil-Nagel A, Strange BA (2016) A fast pathway for fear in human
685 amygdala. *Nat Neurosci* 19:1041-1049.
- 686 Muckli L, De Martino F, Vizioli L, Petro LS, Smith FW, Ugurbil K, Goebel R, Yacoub E (2015)
687 Contextual Feedback to Superficial Layers of V1. *Curr Biol* 25:2690-2695.
- 688 Norris DG, Polimeni JR (2019) Laminar (f)MRI: A short history and future prospects.
689 *Neuroimage* 197:643-649.
- 690 O'Reilly JX, Woolrich MW, Behrens TE, Smith SM, Johansen-Berg H (2012) Tools of the trade:
691 psychophysiological interactions and functional connectivity. *Soc Cogn Affect Neurosci*
692 7:604-609.
- 693 Pajani A, Kok P, Kouider S, de Lange FP (2015) Spontaneous Activity Patterns in Primary
694 Visual Cortex Predispose to Visual Hallucinations. *J Neurosci* 35:12947-12953.
- 695 Pessoa L, Ungerleider LG (2004) Neural correlates of change detection and change blindness
696 in a working memory task. *Cereb Cortex* 14:511-520.
- 697 Pessoa L, Adolphs R (2010) Emotion processing and the amygdala: from a 'low road' to 'many
698 roads' of evaluating biological significance. *Nat Rev Neurosci* 11:773-783.
- 699 Purushothaman G, Marion R, Li K, Casagrande VA (2012) Gating and control of primary visual
700 cortex by pulvinar. *Nat Neurosci* 15:905-912.
- 701 Rahnev D, Maniscalco B, Graves T, Huang E, de Lange FP, Lau H (2011) Attention induces
702 conservative subjective biases in visual perception. *Nat Neurosci* 14:1513-1515.
- 703 Ress D, Heeger DJ (2003) Neuronal correlates of perception in early visual cortex. *Nat Neurosci*
704 6:414-420.
- 705 Roth MM, Dahmen JC, Muir DR, Imhof F, Martini FJ, Hofer SB (2016) Thalamic nuclei convey
706 diverse contextual information to layer 1 of visual cortex. *Nat Neurosci* 19:299-307.
- 707 Saalmann YB, Kastner S (2011) Cognitive and perceptual functions of the visual thalamus.
708 *Neuron* 71:209-223.
- 709 Schwiedrzik CM, Freiwald WA (2017) High-Level Prediction Signals in a Low-Level Area of the
710 Macaque Face-Processing Hierarchy. *Neuron* 96:89-97 e84.
- 711 Shipp S (2003) The functional logic of cortico-pulvinar connections. *Philos Trans R Soc Lond B
712 Biol Sci* 358:1605-1624.
- 713 Shipp S (2007) Structure and function of the cerebral cortex. *Curr Biol* 17:R443-449.
- 714 Shipp S (2016) Neural Elements for Predictive Coding. *Front Psychol* 7:1792.

- 715 Sprenger T, Seifert CL, Valet M, Andreou AP, Foerschler A, Zimmer C, Collins DL, Goadsby PJ,
716 Tolle TR, Chakravarty MM (2012) Assessing the risk of central post-stroke pain of
717 thalamic origin by lesion mapping. *Brain* 135:2536-2545.
- 718 Tamaki M, Bang JW, Watanabe T, Sasaki Y (2016) Night Watch in One Brain Hemisphere
719 during Sleep Associated with the First-Night Effect in Humans. *Curr Biol* 26:1190-1194.
- 720 Tamietto M, de Gelder B (2010) Neural bases of the non-conscious perception of emotional
721 signals. *Nat Rev Neurosci* 11:697-709.
- 722 Tamietto M, Pullens P, de Gelder B, Weiskrantz L, Goebel R (2012) Subcortical connections to
723 human amygdala and changes following destruction of the visual cortex. *Curr Biol*
724 22:1449-1455.
- 725 Torrisi S, Gorka AX, Gonzalez-Castillo J, O'Connell K, Balderston N, Grillon C, Ernst M (2018)
726 Extended amygdala connectivity changes during sustained shock anticipation. *Transl
727 Psychiatry* 8:33.
- 728 Tottenham N, Tanaka JW, Leon AC, McCarry T, Nurse M, Hare TA, Marcus DJ, Westerlund A,
729 Casey BJ, Nelson C (2009) The NimStim set of facial expressions: judgments from
730 untrained research participants. *Psychiatry Res* 168:242-249.
- 731 Van de Moortele PF, Auerbach EJ, Olman C, Yacoub E, Ugurbil K, Moeller S (2009) T1
732 weighted brain images at 7 Tesla unbiased for Proton Density, T2* contrast and RF coil
733 receive B1 sensitivity with simultaneous vessel visualization. *Neuroimage* 46:432-446.
- 734 Willenbockel V, Sadr J, Fiset D, Horne GO, Gosselin F, Tanaka JW (2010) Controlling low-level
735 image properties: the SHINE toolbox. *Behav Res Methods* 42:671-684.
- 736 Witthoft N, Nguyen ML, Golarai G, LaRocque KF, Liberman A, Smith ME, Grill-Spector K (2014)
737 Where is human V4? Predicting the location of hV4 and VO1 from cortical folding. *Cereb
738 Cortex* 24:2401-2408.
- 739
- 740

741

Supporting data

742

743 **Figure 1-1.** Illustration of the differential contribution of anticipation for the HIT and False Alarm (FA)
744 trials. Given that there was no trial-wise cue to forecast the upcoming face stimulus (i.e., fearful or
745 neutral), it is expected that anticipation for the fearful face target was similarly fluctuating across all the
746 trials regardless of the actual type of face stimulus. That is, regardless of the presented face stimulus
747 (fearful or neutral), there are likely to be similar proportions of trials with relatively higher level of
748 anticipation (see inner red circle in the center). When comparing the HIT and FA trials, however,
749 heightened anticipation is likely to contribute to a larger proportion of the FA trials relative to the HIT trials
750 where sensory inputs of presented fearful face also contributed to the percept. This can be inferred when
751 simply considering the proportion of HIT trials that are mainly driven by sensory inputs or alternatively by
752 anticipation. That is, while the proportion of HIT trials ($\approx 55\%$) that is the same as the total FA rate (\approx
753 25%) may be attributed to amplified anticipatory processing, the remaining HIT trials ($\approx 30\%$ out of 55%)
754 is likely to reflect sensory inputs for the target faces instead. Thus, FA trials are more likely to reflect top-
755 down related processing than are HIT trials. Here, trials are binary divided into higher and lower
756 anticipation trials for simplicity, and the actual proportions may vary across participants.

757

758

759

760 **Figure 2-1.** Pulvinar and V1 activity. **A.** Deconvolved time course for the pulvinar for HIT and false alarm
761 (FA) trials during the detection tasks with fearful and happy face targets (left and right panels,
762 respectively). Error bar indicates standard error of mean. **B.** Deconvolved time course of V1 for the HIT
763 and false alarm (FA) trials during the fearful face detection task and happy face detection task (left and
764 right panels, respectively). Error bar indicates standard error of mean. Related to **Figs 2 and 3**.

765

766

767

768
769
770 **Figure 2-2.** Activity of the pulvinar on FA and HIT trials in each of its subregions. **A.** The subregions
771 composing the lateral, inferior, and medial portions of the pulvinar were defined based on a histological
772 atlas (Chakravarty MM et al. 2006). The atlas was imported to BrainVoyager, and the entire pulvinar
773 including all subregions was manually aligned to the pulvinar in each participant's Native space. We
774 included the subregions that compose the lateral, inferior, and medial portions of pulvinar which are
775 widely implicated in visual processing (Pessoa and Adolphs 2010; Bridge et al. 2016), namely the nucleus
776 pulvinaris oromedialis (lateral), nucleus pulvinaris orolateralis (lateral), pulvinar laterale (lateral), nucleus
777 pulvinaris intergeniculatus (inferior), nucleus pulvinaris (medial), and pulvinar mediale (medial). The entire
778 voxels within each subregion were used to estimate the activity level. **B.** Similarly to the results in the
779 Main text (**Fig. 2**) with the functionally defined pulvinar ROIs, there was significantly larger activity on the
780 FA trials of a fearful face relative to the FA trials of a happy face in two subregions, namely the nucleus
781 pulvinaris oromedialis (lateral) and nucleus pulvinaris (medial). However, there was no significant
782 interaction between emotion (fearful/happy) and condition (HIT/FA) in these two subregions (nucleus
783 pulvinaris oromedialis: $F(1,10) = 4.496, p = 0.060$; nucleus pulvinaris: $F(1,10) = 2.327, p = 0.158$). The
784 results suggested that one lateral and one medial subregion showed significantly larger activity on FA
785 trials of a fearful face relative to FA trials of a happy face. Given that the same neutral faces were
786 presented on these trials, the difference in activity is likely to be due to the perceived emotion driven by
787 anticipation of a fearful versus happy face target. These results hint at the possibility that task-driven
788 anticipation of threat signals may be coded in the medial pulvinar through its interaction with the prefrontal
789 areas where task-set is generally represented (Lau and Passingham, 2007), while the lateral pulvinar
790 may directly modulate V1 based on anticipation. However, these results should be treated as indicative
791 as the results within these subregions were limited in that there was no significant interaction between
792 conditions (HIT/FA) and emotions (fearful/happy) and that the relatively lower SNR in the inner brain area
793 like the pulvinar may have interfered with the differentiation of subregion activities (see *Estimation of*
794 *tSNRs*). Box plot shows upper (75%) and lower (25%) quartiles with median (red line) and mean (red dot),
795 with whisker showing maximum and minimum value. An outlier (outside of ± 2.7 standard deviations

796 within a distribution for a given condition) is shown with a red cross. * $p < 0.05$ in planned post-hoc tests. r:

797 right, l: left, a: anterior, p: posterior. Related to **Fig. 2**.

798

799

800

801

802

803

804

805 **Figure 3-1.** V1 activity in each participant at superficial (top row) and deep cortical depths (bottom row).
806 For each subject, deconvolved time course of V1 during the HIT and false alarm (FA) trials during the
807 fearful face detection task and happy face detection task (left and right panels, respectively) are shown.
808 Subjects who showed numerically larger activity on FA trials of a fearful face relative to FA trials of a
809 happy face, which is in line with the pattern of group level result shown in **Fig. 3C**, are highlighted with red
810 fonts (8 out of 11 participants). Related to **Fig. 3**.

811

812

813

814

815

816

817 **Figure 3-2.** The results of gPPI analyses examining the connectivity between the pulvinar and V1. gPPI
818 analyses were separately conducted, with the V1 superficial or deep cortical depth voxels as the seed
819 ROI (see *Generalized form of context-dependent psychophysiological interaction analysis (gPPI)*). Mean
820 t-values for the parameter estimates in gPPI for each trial type and seed ROI are shown. Only during FA
821 trials with fearful faces, a significant modulation of connectivity was present between the pulvinar and V1
822 superficial layers ($t(10) = 3.981$, $p = 0.0026$, one-sample t-test against 0, significant after Bonferroni
823 correction). We note that these results are only indicative, as there was no significant interaction between
824 conditions (HIT/FA), facial emotion (fearful/happy), and V1 cortical depth (superficial/deep) ($F(1,10)=.198$,
825 $p = .666$). There was no evidence that the connectivity between the pulvinar and V1 was modulated
826 during other conditions in either V1 cortical depths. With the V1 superficial cortical depth as a seed ROI,
827 fearful HIT: $t(10) = 0.403$, $p = 0.695$, CI [-0.683 0.985]; fearful FA: $t(10) = 3.981$, $p = 0.0026$, CI [0.319
828 1.128]; happy HIT: $t(10) = 1.869$, $p = 0.091$, CI [-0.105 1.120]; happy FA: $t(10) = 1.4364$, $p = 0.181$, CI [-
829 0.271 1.253]. With the V1 deep cortical depth as a seed ROI, fearful HIT: $t(10) = 0.398$, $p = 0.699$, CI [-
830 0.641 0.92]; fearful FA: $t(10) = 2.223$, $p = 0.05$, CI [-0.001 1.199]; happy HIT: $t(10) = 1.594$, $p = 0.142$, CI
831 [-0.15 0.01]; happy FA: $t(10) = 1.152$, $p = 0.276$, CI [-0.459 1.441]. We note that the null results do not

832 necessarily indicate the absence of effects, because a PPI analysis is generally low in power (O'Reilly et
833 al., 2012) and tSNR in the pulvinar was relatively low in the current study. Future studies may further
834 examine the potential changes in the functional connectivity with the pulvinar across the V1 cortical
835 depths and experimental conditions. pulv: pulvinar, a: anterior, p: posterior.

836

837

838

839

840

841

842

843

844

845

846

847 **Figure 3-3.** Prior to the onsets of target faces, there was already enhanced activity in the pulvinar
848 preceding the false alarm (FA) trial of a fearful face compared with a happy face (left panel). To estimate
849 activity prior to the face onsets, the z-normalised signal change (%) in the preprocessed raw time course
850 (see *fMRI processing*) was averaged between the 2 time points immediately before the face onsets (i.e., -
851 5 and -2.5 s) relative to the preceding baseline (averaged between the 2 earlier time points, i.e., -10 and -
852 7.5 s). A repeated measures ANOVA with two factors of percept type (pre-HIT/pre-FA) and emotion
853 (fearful/happy) revealed a significant interaction ($F(1,10) = 10.094, p = 0.010$). Post-hoc analyses
854 revealed that pulvinar activity was significantly greater on FA trials of fearful faces compared with happy
855 faces in the pre-onset period ($t(10) = 3.392, p = 0.007, d = 1.1$). During the same pre-onset period, while
856 pulvinar activity was significantly larger on HIT than on FA trials of happy faces ($t(10) = 2.386, p = 0.038,$
857 $d = 0.7$), there was a non-significant opposite trend such that activity was relatively greater on FA than on
858 HIT trials of fearful faces ($t(10) = -2.147, p = 0.057$, n.s.). Meanwhile, in the same pre-onset period, there
859 was not yet any differential activity in the V1 superficial cortical depth (right panel), with no significant
860 main effects or interaction between percept type and emotion ($p > 0.50$, n.s.). These results suggest that
861 anticipatory activity in the pulvinar modulated the response of the V1 superficial cortical depth triggered
862 by the subsequent onset of a face target shown in **Fig. 3D**. Box plot shows upper (75%) and lower (25%)
863 quartiles with median (red line) and mean (red dot), with whisker showing maximum and minimum value.
864 ** $p < 0.01$, * $p < 0.05$, + $p < 0.10$. Related to **Figs 2 and 3**.

865

866

867

868

869

870 **Figure 3-4. The results of a control analysis showing no differential activity in the pulvinar and V1**
871 **on MISS versus Correct rejection (CR) trials.** We examined whether similar results on FA trials of
872 fearful faces (**Figs 3B and 4D**) may be present on MISS trials, where a fearful face was presented but
873 was not detected. While the results for FA trials of fearful faces may reflect enhanced top-down
874 processing, other non-mutually exclusive possibilities are worth considering. Specifically, the results for

875 FA trials may reflect a mere mismatch between sensory input and reported percept. Although this
876 possibility is unlikely considering the fact that such results did not generalize to FA trials of happy faces,
877 there remains a possibility that such input-to-percept mismatch may evoke certain neural activity only in
878 anticipation of threat cues. We therefore examined whether the patterns of results we obtained from the
879 contrast between FA and HIT trials may be also obtained from the contrast between MISS and correct
880 rejection (CR) trials, where neutral faces were perceived with or without mismatched sensory input,
881 respectively. **A.** Unlike the contrast of Pulvinar activity between the HIT and false alarm (FA) trials shown
882 in **Fig. 2**, there was no difference in pulvinar activity between the MISS and CR trials regardless of the
883 facial emotion (a non-significant interaction between percept type (MISS/CR) and emotion: $F(1,10) =$
884 0.013, $p = 0.912$). Although we saw a trend for pulvinar activity to be larger for the fearful face detection
885 task than for the happy face detection task, there was no significant main effect of emotion ($F(1,10) =$
886 2.365, $p = 0.155$). **B.** Similarly, unlike the contrast of V1 activity between the HIT and FA trials shown in
887 **Fig. 3**, there was no differential activity in V1 between the MISS and CR trials, regardless of emotion and
888 cortical depth (a non-significant second-order interaction: $F(1,10) = 1.251$, $p = 0.290$). While there was
889 generally greater activity on MISS trials relative to CR trials that was not specific to any facial emotion and
890 potentially reflected sensory inputs of salient emotional faces albeit undetected, there was no significant
891 main effect of percept type ($F(1,10) = 2.573$, $p = 0.140$). Box plot shows upper (75%) and lower (25%)
892 quartiles with median (red line) and mean (red dot), with whisker showing maximum and minimum value.
893 An outlier (outside of ± 2.7 standard deviations within a distribution for a given condition) is shown with a
894 red cross. Related to **Figs 2B and 3D**.

895
896

897

898